

Diffractive optical elements for biomedical applications

Michael Golub, Israel Grossinger
Holo-Or, Ltd, Kiryat Weizmann, P.O.B. 1051, Rehovot 76114, Israel*

ABSTRACT

The set of **diffractive optical elements** for CO₂ and Nd-Yag lasers was theoretically calculated, fabricated by microlithographic technology and experimentally tested. It is shown that the laser systems for therapy, surgery and welding gain from advanced capabilities of the DOEs: uniform focal-spot intensity, simultaneous formation of focal line contours, sharp and multiple-spot focusing, dual-wavelength achromatization, miniaturization. Novel **multifocal diffractive contact lenses** are elaborated based on diffractive microrelief considerations, nonparaxial variant of diffraction integral on curved surface and computer simulations of intensity distribution on eye retina. Tri-focal diffractive contact lenses that were diamond-turned on rigid and soft materials successfully passed tests.

Keywords: diffractive optics, DOE, laser focusing, multifocal lens, contact lens, beam shaping, computer modeling

1. INTRODUCTION

Specific requirements for optics in biomedical applications are not always met by conventional bulky optics. Thus contact and intraocular lenses are supposed to be thin enough and to demonstrate optionally several foci at once. Laser systems for surgery and welding require sharper focusing, convenience of targeting, simultaneous exercising of several points, straight lines or even curved contours, while laser therapy requires uniformly illuminated circular or rectangular area under treatment. Diffractive optical elements (DOEs) open new degrees of freedom in light transformation and offer basically new opportunities for optical systems. Even though DOEs are well known, biomedical applications demand more oriented investigations on light diffraction, materials and tests. The report is based on authors extended experience in design, fabrication and testing of DOEs for ophthalmic and other medical applications. It is divided into two parts: DOEs for medical laser systems and diffractive multifocal contact lenses. Substantially new properties of DOEs are described in comparison with regular optics. Full cycle was performed starting from theoretical optical calculations of DOEs and finishing in their fabrication with experimental investigation. Design approaches for contact lenses are discussed on the base of precise computer simulation of their performance in eye. The calculations we conducted for multifocal diffractive microrelief depth take into consideration such an important factor as local ray direction with respect to surface normal. Novel nonparaxial

simulate intensity distribution on retina of the human eye in the case of diffractive multifocal lens with strict consideration of eye aberrations.

2. DIFFRACTIVE OPTICAL ELEMENTS FOR MEDICAL LASER SYSTEMS

Diffractive lenses for lasers^{1,2} give proper correction of aberrations in stand alone operation as well as in the system with regular refractive lenses. Diffractive lenses with circular Fresnel zones provide only an optical power. They focus collimated laser beam into a spot with the size, determined by aberrations, but do not perform any transformations of the beam. Technology of fabrication of diffractive optical elements (DOEs) naturally gives the possibility to create nonsymmetrical and complicated Fresnel zones of microrelief. The detailed structure of diffractive microrelief zones can be determined from the solution of inverse task for light beam propagation in free space³⁻⁶. We can sort complicated diffractive optical elements into two main classes: beam focusers and beam shapers. Beam focusers demonstrate sharply focused focal image composed from spots and segments of lines. Beam shapers illuminate some part of focal plane with required intensity distribution, for example uniform round or rectangular spot. We list below examples of DOEs that are interesting for medical laser systems and at the same time realistic for implementation.

We concentrated on the following advanced functional capabilities DOEs: aberration correction for sharp focusing of the laser beam, dual-wavelength lenses, beam multiplication towards obtaining several focal spots, parallel formation of focal

* e-mail: holoor@holoor.co.il Telephone: +972 (8) 9409687; Fax: +972 (8) 9409606

line contours without scanning, beam shaping for CO₂ and Nd-Yag lasers to reach uniform intensity distribution. DOEs were fabricated on ZnSe, fused silica. Computer simulations of DOEs performance in laser system were performed on all the stages.

2.1. Diffractively corrected lens

Single lens is attractive for focusing for its simplicity and low cost, but it suffers from aberration and gives relatively large focal spot. **Diffractively corrected focusing lens** is fabricated by etching an *aberrations-correction diffractive microrelief pattern* on the plane side of a bulky spherical plano-convex lens. Diffractive microrelief pattern results in a diffraction-limited spot-size demonstrating a *sharp focusing* effect increased light power density previously expected only from multiple-lens objective.



Fig. 1. Hybrid refractive-diffractive lens with diffractive correction of aberrations

2.2. Dual-wavelength lenses

Further ideas on this way is to use the same lens for two wavelengths that are far away from each other. Most medical CO₂ laser systems employ a HeNe laser for generating a targeting beam. Since the two wavelengths are far apart from each other, the index of refraction of the optics in the beam manipulation system is significantly different for the CO₂ and the HeNe lasers. As a result the HeNe beam is focused closer to the optics than CO₂ laser beam (See Fig. 2) and thus an additional negative lens is required for correcting its location. Conventional methods for introducing this correction make use of combining materials having different optical dispersion.

A very elegant solution to this problem is obtained by using diffractive optics. Diffractive optics opens unique possibilities to affect only one wavelength. By adding a single diffractive surface on one of the ZnSe lenses, it is possible to add the required negative power to the HeNe lens only: due to the considerable difference in wavelength, the CO₂ beam will not be affected by the diffractive surface and thus the two beams will be focused to the same spot as without diffractive microrelief. HeNe beam will coincide with the invisible CO₂ beam (Fig. 3), so that the location of the CO₂ focus will be pointed in advance by low-power visible HeNe laser. This method eliminates the need to employ different materials in the optical system and keeps mechanically one lens in the focusing system. The diffractive surface is etched onto the ZnSe lens itself and thus becomes an integral part of it.

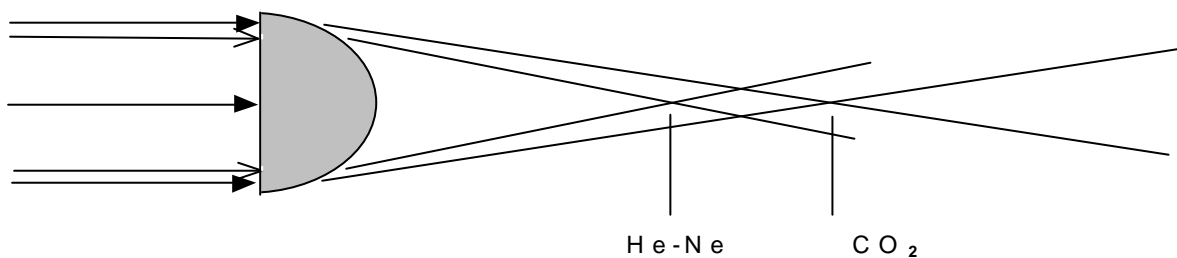


Fig.2. Performance of regular ZnSe lens in dual-wavelength beam of CO₂ and HeNe lasers

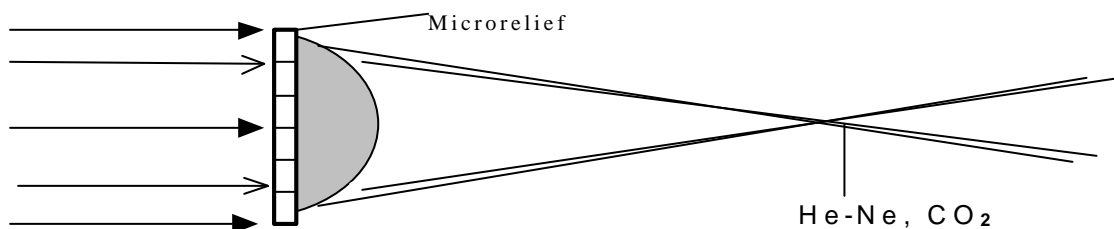


Fig.3. Performance of diffractive-refractive ZnSe lens in dual-wavelength beam of CO₂ and HeNe lasers

2.3. Multifocal lenses

Diffractive optics gives the possibility to create several output beams from one incident beam. Thus instead of one focus it is possible to obtain several foci, located properly on the focal plane. Our experiments confirmed that the structure of each spot is very near to those of well corrected lens.

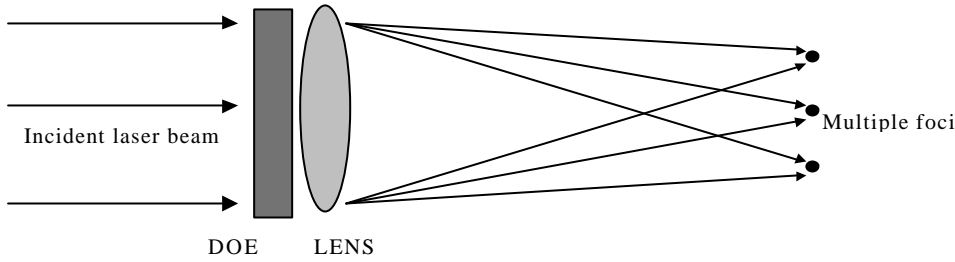


Fig.4. Focusing of the collimated laser beam into several focal spots, laterally separated.

2.4. Beam focusing into focal lines and contours

Going further on this way we can demonstrate continuous set of spots thus giving the line contour. While conventional focusing lens gives a point-spot focus, diffractive focuser that we propose, provides a required caustic line in the focal plane. Our focuser is plano-convex lens with diffractive microrelief pattern on plano surface, directing the laser light towards line-contour (straight line, ring, polygons, letters etc.) instead of single focal spot. Thus a line-contour focal image is got from collimated labeam without any scanning system.

Optically smooth thin phase-only optical element is specified by the smooth phase function $\mathbf{j}(\vec{u})$, where $\vec{u} = (u, v)$ are the transverse coordinates of the point placed on the substrate surface of the optical element. Thus such an element is a direct generalization of diffractive lenses. One example of focal domain is the straight line segment with uniform intensity, formed from gaussian beam. The idea of such an element is simple enough. In dire $\mathbf{j}(\vec{u})$ varies as 1-

$$\mathbf{j}_x(u) = \frac{ka}{IE_A} \cdot \left[u \operatorname{erf} \left(\frac{u\sqrt{2}}{\mathbf{s}} \right) - \frac{\mathbf{s}}{\sqrt{2p}} q^2 \left(\frac{2u}{\mathbf{s}} \right) \right], \quad q(t) = \sqrt{1 - \exp(-t^2/2)} \quad (1)$$

where \mathbf{s} is the parameter of gaussian beam, $2a$ length of the line segment, $k = \frac{2p}{I}$, I - wavelength, E_A -normalizing constant. There is also possibility to get even several lines, composing cross or just rectangular contour (Fig. 5, 6):

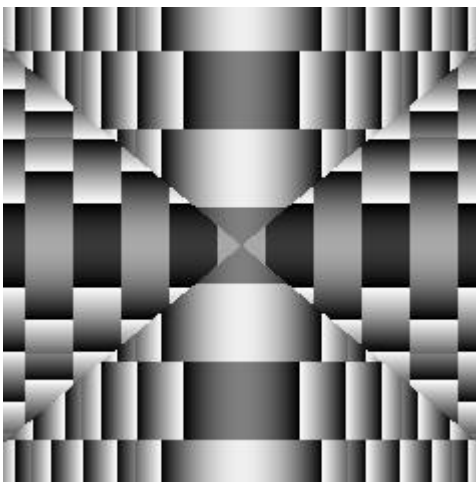


Fig. 5 Grey-level presentation of DOE, focusing into rectangular contour

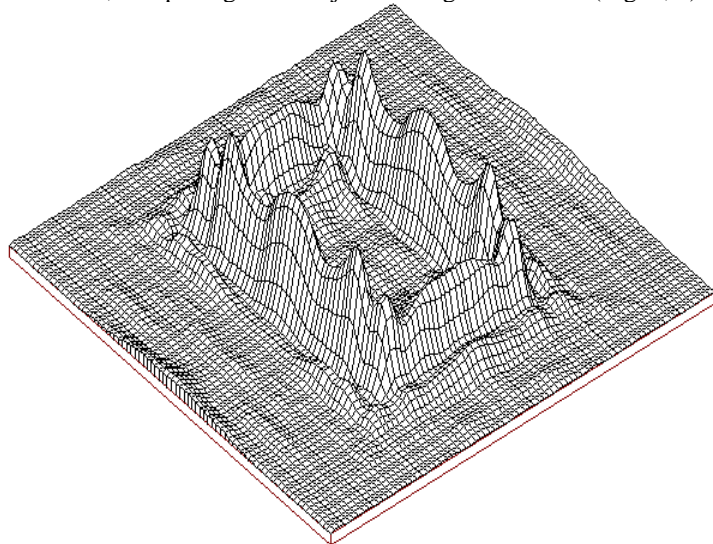


Fig.6. Computer-simulated intensity

The example of the curved-line focus is the ring focuser (Fig. 7). A ray-tracing approach that generalizes the solutions⁴ with respect to the divergence of the incident Gaussian beam, provides an analytical solution for the phase function of the shaper in the form (Fig. 8)

$$\mathbf{j}(r, \mathbf{q}) = k \left[l - \sqrt{l^2 + (r - \mathbf{r}_0)^2} - \mathbf{y}_0(r) \right] + p \mathbf{q} \quad (2)$$

where $\mathbf{j}(u, v) = \mathbf{j}(r, \mathbf{q})$ is the phase function of the shaper, $r = |\mathbf{u}|$ and \mathbf{q} are the polar radius and the polar angle, respectively, for points in the plane of the shaper with cartesian coordinates $\mathbf{u} = (u, v)$, \mathbf{r}_0 is the radius of the ring in the focal plane, and l is the distance between the shaper and the focal plane. p is an integer number, usually $p=0$ or $p=1$. The introduction of this parameter with a value $p=1$ enables a depression of the central peak (Figs. 9, 10).

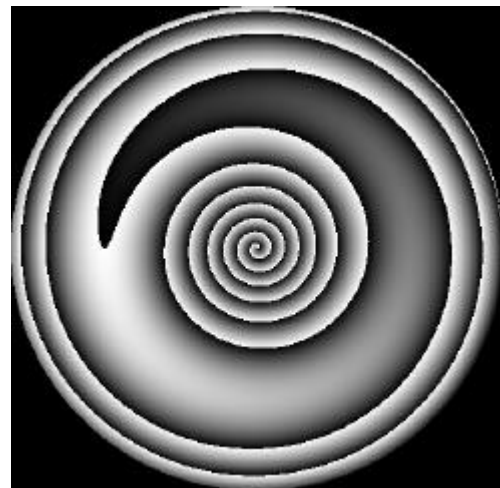
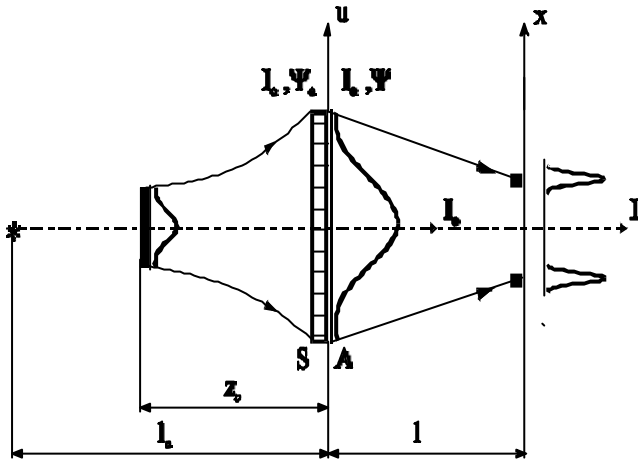


Fig. 7. Geometry of focusing into the ring

Fig. 8. Microrelief of DOE, focusing into ring contour (gray-level presentation)

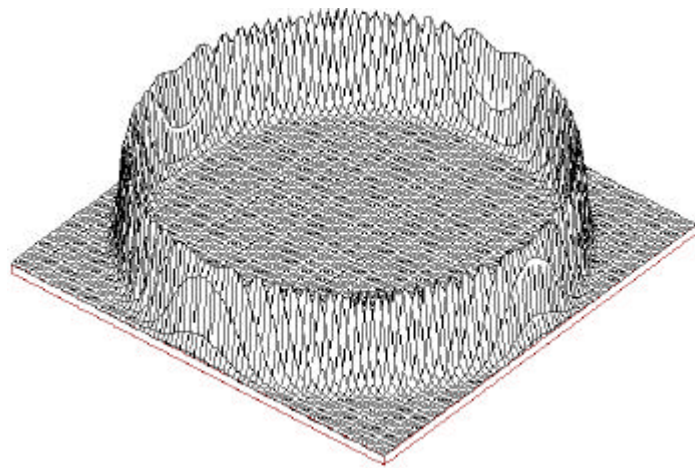
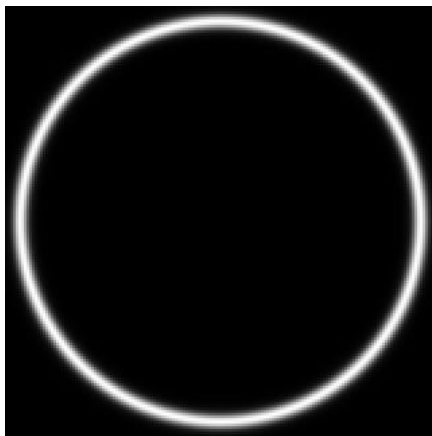


Fig. 9. Computer simulated focal intensity for ring focuser (gray-level presentation)

Fig. 10. Computer simulated focal intensity for ring focuser (3-D graph presentation)

The line-contour focus opens really novel opportunities in laser surgery. We have fabricated several focusers on ZnSe and found their performances very near to theoretical predictions.

2.5. Beam shapers for transforming the intensity patterns of laser beam

Far field patterns of a laser beam often feature the intensity peak at the center, while a more uniform intensity is required in numerous applications. Thus, flattening or reshaping of the near-gaussian laser beam profiles into the top-hat profile (a uniform distribution of intensity over a given spot area) is required. Diffractive optics opens new possibilities for beam shaping by *redistribution of* energy between the center and periphery of the laser beam without any absorbing masks. Diffractive optics technology makes it possible to produce a near gaussian to top-hat transformation by a single beam shaping element with only minimal power losses. This element provides a uniform-spot distribution of specified size and shape at a given distance. In principle any transverse spot shape can be obtained, though the most useful spot shapes are round, rectangular or square shapes with uniform intensity with sharp edges (Fig. 11-13). The integral light transmittance of diffractive beam shapers (75% - 96%) far exceeds those of either slits-

Uniform illumination of the laser light can be useful in laser therapy procedures.

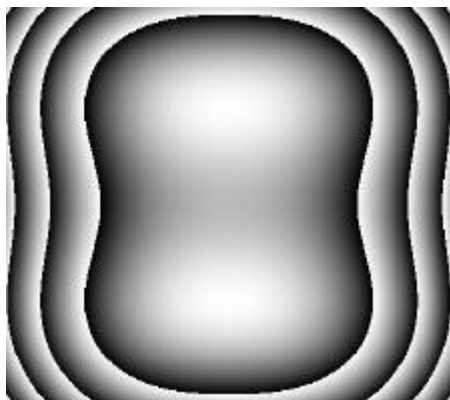
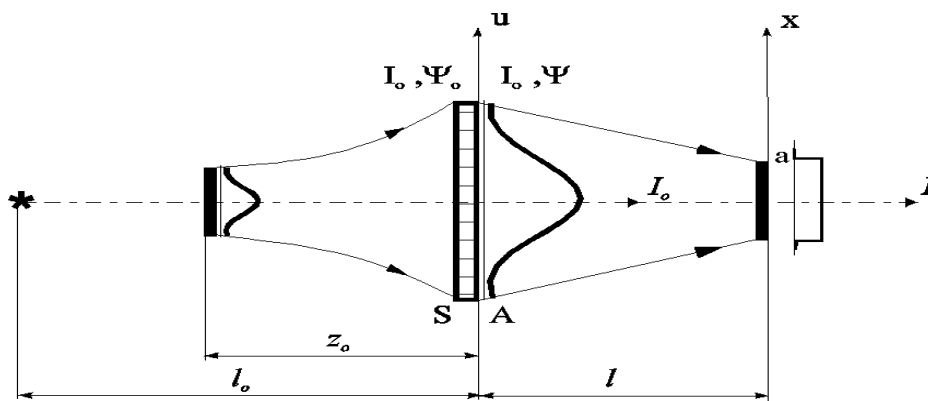


Fig. 12. Gray-level presentation of diffractive shaper

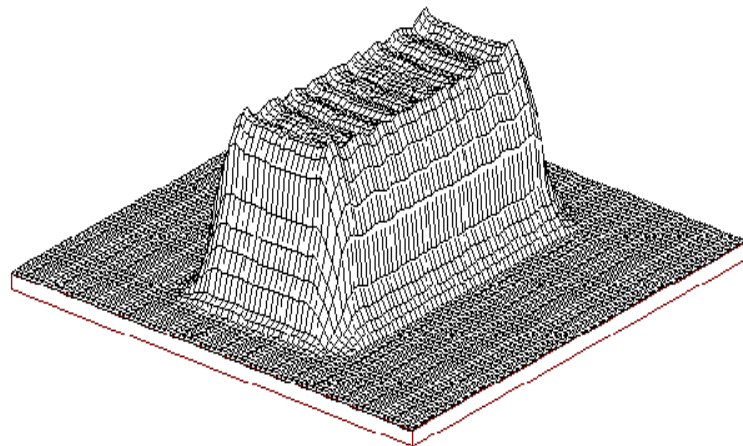


Fig. 13 Computer simulated intensity of the shaped beam

3. DIFFRACTIVE CONTACT LENSES

Multifocal optics helps a lot in solving problems with human eye accommodation abilities. Normal human eye accommodation abilities are ensured by varying optical power of crystalline lens. It is well known that accommodation

abilities usually decrease with age (presbyopia), or can be even lost completely during cataract extraction when crystalline lens is removed et all (aphakia) or substituted by plastic intraocular lens implant (pseudophakia).

Usually bifocal contact lenses are in use ⁷. We report about creation of novel triple-focal contact lenses that provide even more gradual transfer of optical power in accommodation than bi-focal lenses.

3.1 Design of multifocal contact lenses

The triple-focal contact lenses are the hybrid refractive-diffractive component with the three-order diffractive microrelief diamond turned on the curved base surface. Idea of correction of eye accommodation abilities is to create three foci along the optical axis. Each focus works for the proper object so that only one focus provide an image on the retina for a given object distance (see Fig. 14). For example (-1) diffraction order of the lens with negative optical power works for far object, (0) order with zero optical power works for middle object and (+1) order with positive optical power works for near object as illustrated. Unused diffraction orders together with higher orders contribute to defocused images that reduce the contrast of the usefull image b

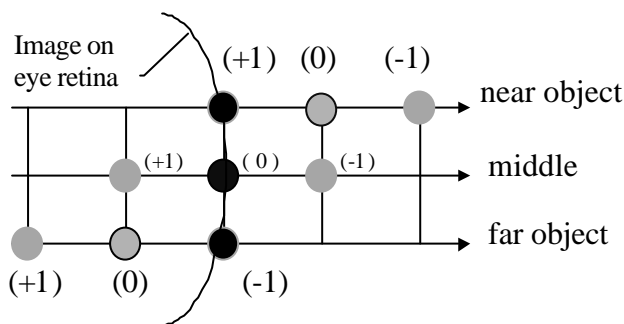


Fig. 14. Several focuses and the image

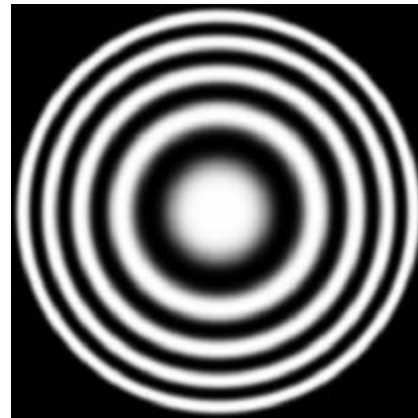


Fig. 15. Diffractive microrelief of trifocal lens

Triple- focal operation for contact lens is achieved by adding the diffractive microrelief pattern (see Fig. 15) on one of the smooth optical surfaces. Smooth optical surfaces ensure prescribed optical power for middle-distance object while diffractive microrelief works for far and near object. Contact lens is mechanically rather complicated structure with front and base surface and edge (Fig.16). Front surface include optical zone, lenticular zone. Base surface feature optical zone with diffractive grooves and periphery. It gives three foci under illumination by each of type objects: far, middle, near.

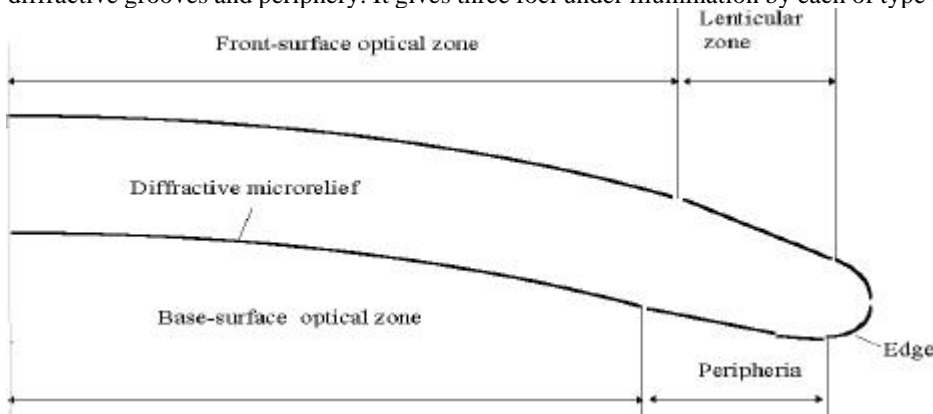


Fig. 16. Scheme of multifocal contact lens (not in scale)

3.2. Diffraction on curved substrates with microrelief

Important problem in contact lens design is to predict its performance before fabrication by computer simulation of intensity on retina of the eye. It is also desired to know what parameters should be expected from contact lens in measuring system during optical testing of finished contact lenses. We have to know exactly not only position of three foci and their spot-sizes but also the light beam power distribution between foci, peak intensity in each focus. There are series of papers

dedicated to computer simulation of diffractive optical elements, for example⁸, by Fourier and Fresnel transform that use plane substrate surface. Diffractive contact lenses however demonstrate several special features:

- diffractive microrelief is on the curved surface, while usually DOEs have planar substrate;
- radius of curvature of the substrate is comparable to the diameter of the optical zone of contact lens;
- nonparaxial diffraction integral to be calculated, while usually paraxial Fresnel transform is used;
- ray-tracing done in one working diffraction order, but the output image power is contributed by several diffraction orders;
- the properties of incident beam must be defined on the curved surface, not on its cross-section by plane.

The problem with diffraction orders is the following. Diffractive microrelief is usually described by its special phase function for each diffractive order. Then each order is treated separately by ray-tracing in routine way⁹ without consideration for any interaction between diffraction orders. So far, defocused images of other orders will not be superimposed on the order of interest in this simulation. For proper description of all orders we must really describe diffraction on microrelief. But for this we must interrupt ray tracing on the surface with microrelief. The problem arises: how to know the illuminating beam phase just before the microrelief surface and how to describe multiple beam transformation after its diffraction on microrelief. In other words, the surface with diffractive microrelief is only one of the surfaces in ray-tracing approach, but this particular surface becomes a surface of special attention for all diffractive calculations. We suggest to bring all results of long ray tracing to one surface with given phase function on it.

Thus our general idea of simulation is to bring all the optical surfaces before and after diffractive microrelief to one surface to get regular Kirchhoff diffraction integral applicable. In other words we get equivalent optical scheme for estimation of multifocal diffractive lens. The surfaces before diffractive microrelief are already treated by illuminating beam model. The surfaces after diffractive microrelief have to be reduced now to one surface by the special trick described below.

Λ . It means the complex amplitude of a light field taken on the curved surface, that plays a role of substrate for microrelief (See Fig. 17). In complicated multi-surface optical system illuminating beam is not spherical. It is image of spherical beam formed through all the surfaces, located before microrelief (in the direction of light propagation). Most important characteristic of illuminating beam is the eikonal on the surface Λ with diffractive microrelief. It is desired that the eikonal of nearest spherical beam is subtracted from illuminating beam, because Kirchhoff integral in the form we will use provides its own care about best fitting spherical beam. Thus we have a task of extracting illuminating beam eikonal from conventional ray-tracing program. The

on Λ just before microrelief. This surface has zero thickness but supplies a phase jump. The polynomial coefficients of such a phase jump are chosen so that to compensate all the differences from ideal spherical beam. This goal is achieved by optimization with RMS or peak-value criteria on wavefront near surface Λ ; optimization variables are simply the polynomial coefficients of phase jump on surface Λ . It should be mentioned that the radius of the best-fitting sphere is chosen before optimization. One of the ways to choose that radius is to make zero coefficient of second power polynomial for very little paraxial diameter of optical system. Other way is to find best RMS focus position and treat it as a position of center of best-fitting sphere.

Treating the surfaces after diffractive microrelief features multiple beams and should be considered within diffraction model. After determination of illuminating beam and calculating Kirchhoff integral we will have some complex amplitude $w_{int}(\mathbf{x}_{int})$ distribution that is an intermediate image of object through the part of optical system that contains surfaces before microrelief and microrelief itself. The rest surfaces of optical system will re-image (with some scale V) the intermediate image into final image with complex amplitude $w_{out}(\mathbf{x})$ where \mathbf{x} are the 2-D Cartesian coordinates in the output image plane of all the system. From the point of view of imaging systems the function $w_{int}(\mathbf{x}_{int})$ describes extended source whose image is a convolution:

$$w_{out}(\mathbf{x}) = \int w_{int}(\mathbf{x}' / V) h_{rest}(\mathbf{x} - \mathbf{x}') d^2 \mathbf{x}' \quad (3)$$

where $h_{rest}(\mathbf{x})$

$w_{int}(\mathbf{x}' / V)$ - complex amplitude after diffraction brought to the scale of the output image.

In Fourier domain the convolution takes form:

$$w_{out}(\mathbf{x}) = \int W_{out}(\mathbf{n}) \exp(i2\pi \mathbf{n} \cdot \mathbf{x}) d^2 \mathbf{n} \quad (4)$$

$$W_{out}(\mathbf{n}) = W_{int}(\mathbf{n}) H_{rest}(\mathbf{n}), \quad H_{rest}(\mathbf{n}) = \int h_{rest}(\mathbf{x}) \exp(-i2\mathbf{p}\mathbf{x}) d^2\mathbf{x} \quad (5)$$

$$W_{int}(\mathbf{n}) = \int w_{int}(\mathbf{x}'/V) \exp(-i2\mathbf{p}\mathbf{x}') d^2\mathbf{x}' \quad (6)$$

where $H_{rest}(\mathbf{n})$ after diffractive microrelief. The

problem of finding $w_{out}(\mathbf{x})$ is brought to the problem of calculating Fourier Transform of $w_{int}(\mathbf{x}'/V)$. It is important to mention that function $w_{int}(\mathbf{x}'/V)$ can be treated as an ideal paraxial image of object with complex amplitude $w_{int}(\mathbf{x})$. If we will add the imaging phase on surface Λ so that to ensure scale V then instead of $w_{int}(\mathbf{x}'/V)$ we will obtain directly $w_{int}(\mathbf{x})$ without any special care. This means that illuminating beam in Kirchhoff integral should be without spherical beam but the parameter of distance l for Kirchhoff integral calculation should be chosen so that to ensure scale V .

In accordance with sine-theorem of geometrical optics the scale at two stages of optical system will be the same if the numerical apertures are the same. Thus for calculation of Kirchhoff integral (See Fig. 19) we must take the refractive index n_{kirch} that is equal to the refractive index n_{out} in the image plane of optical system and also keep the same aperture angle. Finally all the multi-surface optical system (See Fig. 17) is substituted by equivalent optical system (See Fig. 18) with one surface Λ and diffractive microrelief on it. The phase on Λ is the sum of phase of illuminating beam, phase jump of diffractive microrelief, phase of coherent transfer function $H_{rest}(\mathbf{n})$ and phase for ideal imaging.

The algorithm described above gives us possibility to reduce multi-surface optical system with diffractive microrelief and spherical illuminating beam to the one-surface optical system with the same microrelief but special aspheric illuminating beam. The internal distances of such an optical system are different from those in original system, but the scale and shape of image in output plane are exactly the same. At the same time reduced or equivalent optical system gives the possibility to apply directly Kirchhoff integral for the system with diffractive microrelief.

The algorithm presented is rather complicated, but it can be considerably simplified by exploiting such a reason: optical path difference characterize the difference from spherical beam at any place of optical system. Travelling along optical system between two neighboring surfaces changes only the scale of coordinates not the values of optical path difference or phase. Thus instead of phase of coherent transfer function of the rest system we can use phase corresponding to optical path difference through that rest part of optical system. But the illuminating beam was characterized by optical path difference for the initial part of optical system (before microrelief). Thus on the surface Λ with microrelief we have all the optical path difference through optical system. The simplified algorithm appears now in such a form:

Algorithm for building equivalent scheme for multifocal aberrated optical system

Ray-trace original optical system (Fig. 16) with diffractive microrelief characterized by phase function (by standard ray-tracing software)

Find the **corrective** polynomial **aberration** coefficients on Λ so that **multi-lens ray-tracing** in given diffraction order gives ideal imaging from input object (far, middle or near) to the output spot

In **equivalent scheme summarize** the phase on the surface Λ from inverse sign **corrective** coefficients with the phase of **diffractive** microrelief in given order

Set distance l so that output numerical aperture **b** of equivalent system is equal to those of multi-lens s

Calculate Kirchhoff integral from surface Λ to the focal domain of interest, at a distance l where the output numerical aperture of equivalent system is equal those of original system (Fig.19).

Thus we are able to deal with equivalent model of diffractive microrelief performance. This means that there is only one surface Λ with diffractive microrelief of variable height h . Contribution of all other optical surfaces is taken into kS_0 and intensity distribution I_0 on the diffractive surface Λ as was described above.

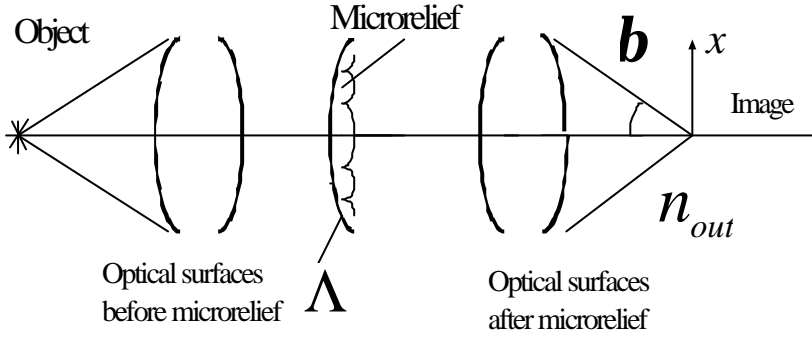


Fig. 17. Original multifocal aberrated optical systems diffraction

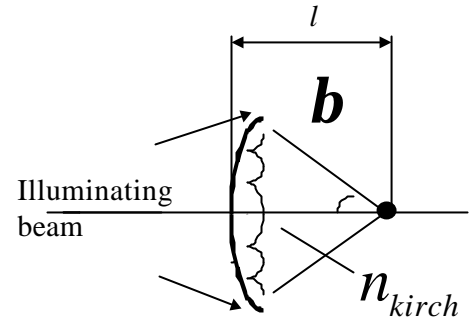


Fig. 18. Equivalent scheme for diffraction

We will use Cartesian 3D coordinate system centered at the vertex O of surface Λ with z denote $\mathbf{u} = (u, v)$ transverse Cartesian coordinates of the current point (\mathbf{u}, H) on the surface Λ , where $z = H(\mathbf{u})$ is the equation for surface Λ . Refractive index n_{kirch} of the media after the surface Λ is given. Phase function $\Phi(\mathbf{u})$ of diffractive microrelief is also given as a phase jump on the surface Λ .

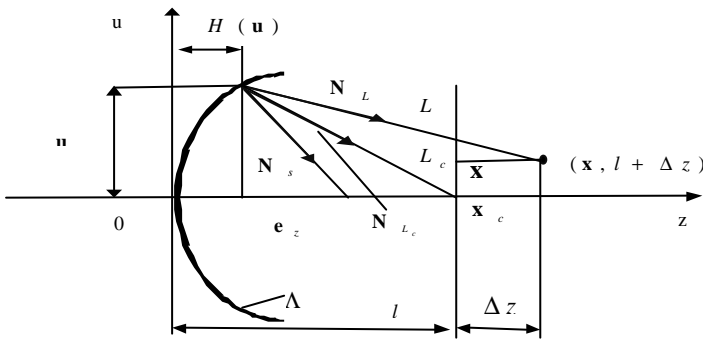


Fig. 19. Detailed scheme for diffraction on curved surface

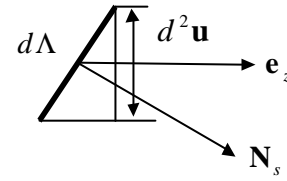


Fig. 20. Tilt of the element of curved surface

We suppose that the light field is concentrated around some center of observation with coordinates (\mathbf{x}_c, l) . The task is to calculate light field w not only exactly at the point (\mathbf{x}_c, l) but also for points $(\mathbf{x}, l + \Delta z)$ in vicinity (See Fig. 19) using general Kirchhoff integral, that is well applicable here due to rather wide zones if compared with:

$$w(\mathbf{x}, l + \Delta z) = \frac{kn}{2\pi i} \int w_c(\mathbf{u}, H(\mathbf{u})) \frac{\exp(iknL)}{L} \mathbf{K}(\mathbf{u}, \mathbf{x}_c, \Delta z) d\Lambda \quad (7)$$

where: w_c - light field just before the curved surface, L - distance from point on the surface Λ to the watching point,

$\mathbf{K}(\mathbf{u}, \mathbf{x}_c, \Delta z) = 0.5 \{ \mathbf{N} \mathbf{N}_s + \mathbf{N}_L \mathbf{N}_s \}$ - tilt factor,

$d\Lambda = \sqrt{1 + |\nabla_{\perp} H|^2} d^2 \mathbf{u}$, - element of square on the surface Λ (See Fig. 20), $\nabla_{\perp} = \left(\frac{\partial}{\partial u}, \frac{\partial}{\partial v} \right)$ - gradient with respect

to coordinated (u, v) , \mathbf{N}_s - unit normal vector of the surface Λ , \mathbf{N} - ray unit vector after diffractive microrelief, \mathbf{N}_L - unit vector pointing towards the observation center from the point on the surface Λ , $k = 2\pi / \lambda$, λ - wavelength.

In such general form

transform as it is usually done for Fresnel transform under paraxial approximation. But along with complexity of non-paraxial and curved surface we have here a small parameter: size of image of the point source. Once the optical system is imaging, the

spot size is small compared to the focal length - spot approximation for light diffraction on microrelief located on curved radial symmetrical substrate and substitution of variables we brought the Kirchhoff integral to single Fourier transform. The substitution is nonlinear, because the distances depend on \mathbf{u} . The intensity eikonal, and phase function can be any nonsymmetrical.

$$w(\mathbf{x}, l + \Delta z) = \sqrt{\frac{E_{sph}}{S_{sph}}} \frac{\mathbf{l} \exp(ikn_{kirch}\Delta z)}{n_{kirch}i} \int \sqrt{I_0(\mathbf{u})} \exp[ikS_0(\mathbf{u}) + i\Phi(\mathbf{u})] K(\mathbf{u}, 0, \Delta z) \frac{L_{c\Delta z}^3}{L_c l_H} \frac{\sqrt{1 + |(H')|^2}}{|l_H + r - H|} \exp[-i2\mathbf{p} \frac{\mathbf{l}}{n_{kirch}} \frac{L_{c\Delta z}^2}{2f_{def}(\mathbf{u}, \Delta z)} \mathbf{n}^2] \exp[i2\mathbf{p} \mathbf{n} \mathbf{x}] d^2 \mathbf{n} \quad (8)$$

E_{sph} - total power of illuminating spherical beam converging into the center \mathbf{x}_c of watching points

S_{sph} - square of the sphere with radius l within the optical aperture of base surface,

$$L_c = \sqrt{[l - H(\mathbf{u})]^2 + (\mathbf{x}_c - \mathbf{u})^2}, \quad L_{c\Delta z} = \sqrt{(l + \Delta z - H(\mathbf{u}))^2 + (\mathbf{x}_c - \mathbf{u})^2}, \quad l_H = l - H + \Delta z \quad (9)$$

Spatial frequencies and coordinates:

$$\mathbf{n} = \frac{n_{kirch}}{\mathbf{l}} \frac{\mathbf{u}}{L_{c\Delta z}}; \quad \mathbf{n} = \frac{n_{kirch}}{\mathbf{l}} \frac{r}{\sqrt{l_H^2 + r^2}} \mathbf{n} = |\mathbf{n}|, \quad r = |\mathbf{u}| \quad (10)$$

$$\text{Equivalent focus: } f_{def} = \frac{(l_H + L_{c\Delta z})(l - H + L_c)}{2\Delta z \left[1 + \frac{l + \Delta z/2 - H}{(L_{c\Delta z} + L_c)/2} \right]} \quad (11)$$

Tilt factor

$$K = \frac{\frac{\mathbf{l}}{n_{kirch}} v H' + \sqrt{1 - \frac{\mathbf{l}^2}{n^2} v^2} + \frac{l_H}{L_c} \frac{\mathbf{l}}{n_{kirch}} v H' + \frac{l - H}{L_c}}{2\sqrt{1 + (H')^2}} \quad (12)$$

- derivative of H with respect to r .

Equation (8) gave us possibility towards computer simulation in the case of curved nonparaxial surface of contact lens. All the algorithms were implemented as the programs written by the author in C++ object-oriented programming language. Some of the results of simulation are presented on the pictures Fig. 21-22. It can be seen that three foci take occur at once, with proper scale of intensity for each.

3.3. Fabrication and tests for multifocal contact lenses

Based on design and simulation results presented above several samples of multifocal contact lenses were fabricated on rigid and soft-type plastic materials by single-path diamond-turning. The bridge between design issues and real diamond-turning machine is created by software program that generate files of diamond tip toolpath depending on parameters of given contact lens. The diamond turning software have been elaborated especially that differs from general diffractive optics software¹⁰ in

terms of edge and also diffractive microrelief type. The files are generated in CNC or similar formats that are acceptable by Rank Pneumo, Precitech and other lathes.

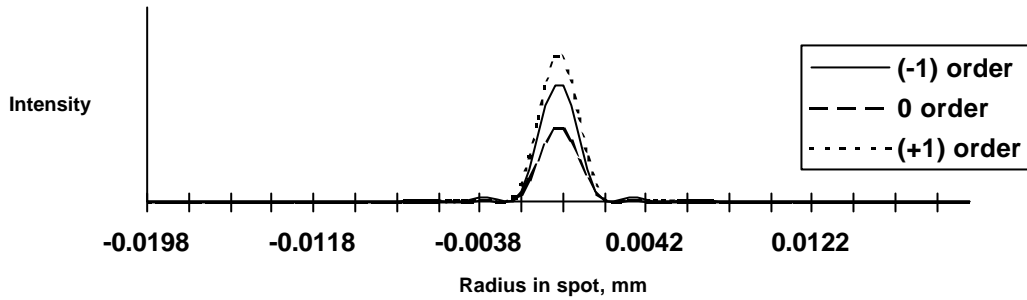


Fig. 21. Simulated focal intensity distribution in multifocal lens

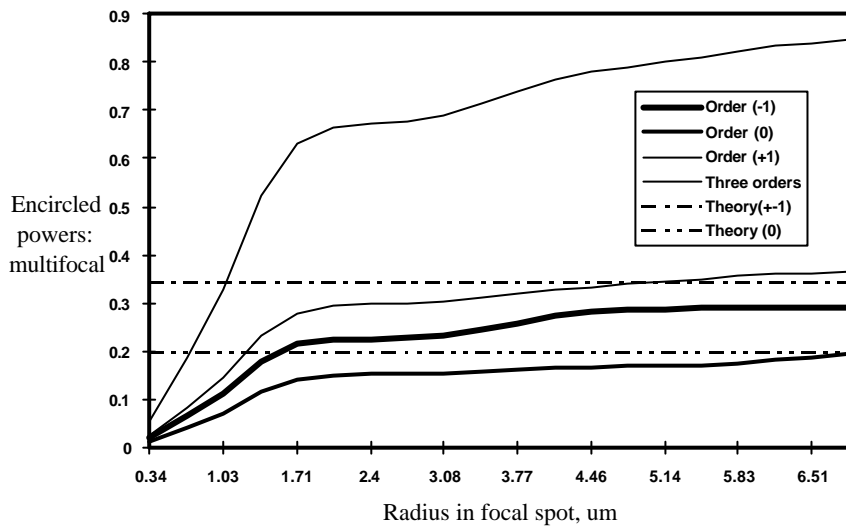


Fig. 22. Encircled powers for multifocal lens simulation in eye model (4 mm diameter)

Real diamond-turned contact lens are shown in the presentation. The tests of contact lenses were done in modified lensometer that measure optical power of each focus and also a relative peak intensity in each focus. Relative peak intensity gives the estimation of energy efficiency of contact lens and estimation of energy distribution between foci. It can be seen from the Tables 1, 2 that the results of measurements are in a good agreement with theoretical input.

Table. 1. Data for rigid contact lens, fabricated on Boston ES material. Theoretical energy distribution (%) between three foci 40.1 / 19.8 / 40.1; Diffraction orders (-1) / (0) / (+1) correspond to far, middle, near object.

Lens	Measurements			Computer simulation		Theory	
	Optical power, D, (-1)/(0)/(+1)	Energy distribution %, (-1)/(0)/(+1)	Effic. %	Energy distribution %, (-1)/(0)/(+1)	Effic. ,%	Optical power, D, (-1)/(0)/(+1)	BC, mm
1	-7.14/-5.96/ -4.73	42.5 / 17.0 / 40.5	83	41.0 / 20.8 / 38.2	88.9	-7.25/-6.00/ -4.75	7.7
2	-7.00/-5.85/ -4.56	42.0 / 18.0 / 40.0	85			-7.25/-6.00/ -4.75	7.7
3	-6.51/-5.29/ -4.03	41.0 / 17.0 / 42.0	81			-6.5/-5.25/ -4.00	7.6
4	-6.38/-5.21/ -3.94	40.5 / 18.0 / 41.5	83			-6.5/-5.25/ -4.00	7.6

Table 2. Data for soft contact lens, fabricated on BENZ45 material, theoretical energy distribution (%) between three foci 40.1 / 19.8 / 40.1. Diffraction orders (-1) / (0) / (+1) correspond to far, middle, near object.

Lens	Measurements			Computer simulation		Theory	
	Optical power, D, (-1)/(0)/(+1)	Energy distribution %, (-1)/(0)/(+1)	Effic. %	Energy distribution %, (-1)/(0)/(+1)	Effic. %	Optical power, D, (-1)/(0)/(+1)	BC, mm
1	-2.92/-1.72/-0.43	39.5 / 21.0 / 39.5	86	41.0 / 20.8 / 38.2	88.9	-3.00/-1.75/-0.50	8.7
2	-2.88/-1.71/-0.39	37.5 / 21.0 / 41.5	88			-3.00/-1.75/-0.50	8.7
3	-3.13/-1.94/-0.65	39.5 / 21.0 / 39.5	85			-3.00/-1.75/-0.50	8.7
4	-3.03/-1.82/-0.51	40.5 / 19.0 / 40.5	83			-3.00/-1.75/-0.50	8.7
5	-2.94/-1.74/-0.46	38.0 / 21.0 / 41.0	83			-3.00/-1.75/-0.50	8.7

Data on clinical results presented in the paper ¹¹ proves the concept of diffractive triple-focal contact lenses and their convenience in the cases of presbyopic and aphakic eyes.

REFERENCES

- Opt. Eng.* **1** (5), pp. 791-795, 1985
2. N. Davidson, A. A. Friesem, Hasman, E. "Analytic design of hybrid diffractive-refractive achromats", *Appl. Opt.* **32**(25), pp. 4770-4774, 1993,
 3. M.A. Golub, I.N. Sisakyan, V.A. Soifer, "Infrared radiation focusators," *Optics and Lasers in Engineering* **15** (5), pp. 297-3, 1991
 4. L. L. Doskolovich, S.N. Khonina, V.V. Kotlyar, I. A. Nikolsky, V.A. Soifer and G.V. Uspleniev, "Focusators into a ring" *Optics and Quantum Electronics* **25**, 801-814, 1993.
 5. C.C. Aleksoff, K.K. Ellis, B.D. Neagle, "Holographic Conversion of a Gaussian Beam to a Near-field Uniform Beam," *Opt. Eng.* **30** (5), pp. 537-543, 1991.
 6. M.A. Golub, M. Duparre, E.B. Kley, R. Kowarschik, B. Luedge, W. Rockstroh, H.-generated diffractive beam shaper for flattening of single-mode CO₂ - *Opt. Eng.* **35**(5), 1400-1406, 1996.
Holographic Optics: Optically and computer generated, Proc. SPIE, 1052, pp.142-149, 1989
- Appl. Opt.* **33**(7), pp. 1135-1140, 1994
- Appl. Opt.* **32**(25), pp. 4775-4784, 1993
10. C.G. Blough, M. Rossi, S.K. Mack, R. -point diamond turning and replication of visible and near-
Appl. Opt. **36**(20), pp. 4648-4654, 1997
- Or trifocal di *The Contact Lens Association of Ophthalmologists Journal* **22**(4), pp. 245-249, 1996